

# Effects of finite coverage on global polarization observables in heavy ion collisions

Shaowei Lan<sup>1</sup>, Zi-Wei Lin<sup>1,2</sup>, Shusu Shi<sup>1</sup>, Xu Sun<sup>1</sup>

<sup>1</sup>*Key Laboratory of Quarks and Lepton Physics (MOE) and Institute of Particle Physics, Central China Normal University, Wuhan, 430079, China and*

<sup>2</sup>*Department of Physics, East Carolina University, Greenville, North Carolina 27858, USA*

In non-central relativistic heavy ion collisions, the created matter possesses a large initial orbital angular momentum. Particles produced in the collisions could be polarized globally in the direction of the orbital angular momentum due to spin-orbit coupling. Recently, the STAR experiment has presented polarization signals for  $\Lambda$  hyperons and possible spin alignment signals for  $\phi$  mesons. Here we discuss the effects of finite coverage on these observables. The results from a multi-phase transport and a toy model both indicate that a pseudorapidity coverage narrower than  $|\eta| < \sim 1$  will generate a larger value for the extracted  $\phi$ -meson  $\rho_{00}$  parameter; thus a finite coverage can lead to an artificial deviation of  $\rho_{00}$  from  $1/3$ . We also show that a finite  $\eta$  and  $p_T$  coverage affect the extracted  $p_H$  parameter for  $\Lambda$  hyperons when the real  $p_H$  value is non-zero. Therefore proper corrections are necessary to reliably quantify the global polarization with experimental observables.

*Introduction.* The dense matter created in non-central relativistic heavy ion collisions processes a large orbital angular momentum. It has been predicted that the orbital angular momentum may result in a net-polarization of produced particles along the direction of the initial angular momentum due to the spin-orbit coupling [1, 2]. Recently, the RHIC-STAR collaboration claimed the discovery of a global  $\Lambda$  polarization in heavy ion collisions [3]. The estimated vorticity is much larger than all other known fluids, which suggests that the quark-gluon plasma is the most vortical fluid produced in the laboratory. Meanwhile the measured spin alignment parameter  $\rho_{00}$  of  $\phi$  mesons is systematically larger than  $1/3$  [4, 5]. A deviation of  $\rho_{00}$  from  $1/3$  indicates a spin alignment of the vector mesons, and whether  $\rho_{00}$  is greater or smaller than  $1/3$  depends on the hadronization mechanism [2]. More detailed measurements of polarization observables, e.g., as a function of rapidity, pseudorapidity ( $\eta$ ), or transverse momentum ( $p_T$ ), will be important to better understand the novel polarization phenomena.

The angular distribution of the  $\Lambda$  decay products with respect to the orbital angular momentum of system  $\mathbf{L}$  can be written as [6]

$$\frac{dN}{d\cos\theta^*} \propto 1 + \alpha_H p_H \cos\theta^*, \quad (1)$$

where  $\theta^*$  is the angle between  $\mathbf{L}$  and the momentum of the daughter proton in the rest frame of the parent  $\Lambda$  hyperon, and  $\alpha_H$  is the decay parameter  $\alpha_\Lambda = -\alpha_\Lambda = 0.642 \pm 0.013$  [7]. Therefore the global polarization parameter  $p_H$  for  $\Lambda$  can be calculated by

$$p_H = \frac{3}{\alpha_H} \langle \cos\theta^* \rangle. \quad (2)$$

The angle brackets above represent the averaging over all  $\Lambda$  decays. Assuming a perfect detector acceptance, one can also write [8]

$$p_H = \frac{8}{\pi\alpha_H} \langle \cos(\phi_p^* - \phi_{\mathbf{L}}) \rangle, \quad (3)$$

where  $\phi_p^*$  is the azimuth of the daughter proton momentum vector in the  $\Lambda$  rest frame and  $\phi_{\mathbf{L}}$  is the azimuth of the system angular momentum.

For vector mesons such as the  $\phi$  meson, the polarization information including the spin alignment is described by a spin density matrix  $\rho$ . A deviation of the diagonal element  $\rho_{m,m}$  ( $m = -1, 0, 1$ ) from  $1/3$  is the signal of spin alignment. For a diagonal matrix  $\rho$ , since the elements  $\rho_{-1,-1}$  and  $\rho_{1,1}$  are degenerate,  $\rho_{0,0}$  is the only independent element [9]. It can be extracted from the following angular distribution of the decay products of vector mesons with respect to  $\mathbf{L}$  [10]:

$$\frac{dN}{d\cos\theta^*} \propto (1 - \rho_{00}) + (3\rho_{00} - 1) \cos^2\theta^*. \quad (4)$$

So far lots of theoretical progresses have been made on the evolution of vorticity and polarization [11–14]. Since the experimental coverage of the phase space is always finite, in this paper we study the effects of a finite  $\eta$  and  $p_T$  coverage on the measured global polarization parameter  $p_H$  of  $\Lambda$  hyperons and spin alignment parameter  $\rho_{00}$  of  $\phi$  mesons.

*The simulation method.* We have modified a multi-phase transport (AMPT) model [15] for this study. The string melting version of the AMPT model [16] used here consists of a fluctuating initial condition, an elastic parton cascade, a quark coalescence model for hadronization, and a hadron cascade. We use the same model parameters as those used for the top RHIC energy in an earlier study [17]. In the hadron cascade of AMPT,  $\phi$  mesons and  $\Lambda$  hyperons are assumed to be uniformly polarized according to Eqs.(1) and (4) when they decay. The included channels of polarized decays are  $\phi \rightarrow K + \bar{K}$  (branching ratio  $\sim 83\%$ ) and  $\Lambda \rightarrow p + \pi^-$  and  $n + \pi^0$  (branching ratio  $\sim 100\%$ ). While experimentally the direction of the angular momentum is often estimated by the normal of the reconstructed event plane [8, 9], we directly calculate the initial angular momentum vector of the participant nucleons event-by-event in the AMPT calculations. All results in this study are for minimum

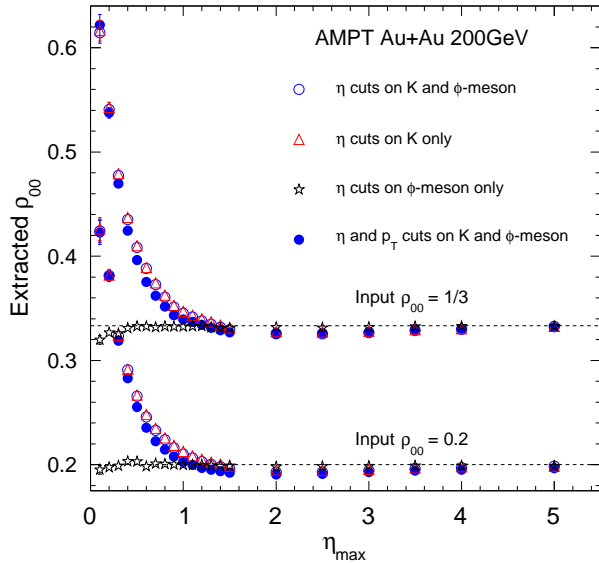


FIG. 1. (Color online) The extracted  $\rho_{00}$  as a function of the upper limit of the  $|\eta|$  coverage from AMPT for minimum bias Au+Au collisions at  $\sqrt{s_{NN}} = 200$  GeV, where dashed lines represent the input  $\rho_{00}$  value of 0.2 or  $1/3$ . Results for  $\eta$  cuts applied to both kaons and  $\phi$  mesons, only kaons, and only  $\phi$ -mesons are shown, in addition to results with both the  $\eta$  cuts and the STAR  $p_T$  cuts on kaons and  $\phi$ -mesons.

bias (impact parameter from 0 to 15.6 fm) Au+Au collisions.

We follow the experimental procedure to extract the  $\rho_{00}$  parameter of  $\phi$  mesons: pairs of  $K\bar{K}$  from each event are used to reconstruct the  $\phi$ -meson candidates, while pairs from different events are constructed to estimate the background; these same event pairs and mixed event pairs are both divided into multiple  $\cos\theta^*$  bins. We then extract the  $\rho_{00}$  parameter by using Eq. (4) to fit the  $|\cos\theta^*|$  distribution of the  $\phi$ -meson signal, i.e., the difference between the same event and mixed event pairs. For  $\Lambda$  hyperons, we found that the systematic uncertainty of background subtraction (up to a fraction of a percent) is too large when the input  $p_H$  is small or zero; it is also not straightforward to apply topological cuts to decays from the AMPT model as done in the experimental analysis. Therefore we use the  $\Lambda$  decay information from the AMPT model directly to extract the  $p_H$  parameter. We have found that hadronic rescatterings have negligible effects on the value of the extracted  $p_H$  parameter for  $\Lambda$  hyperons or the  $\rho_{00}$  parameter for  $\phi$  mesons; this is expected due to their long lifetimes before decay. We have also used the  $\phi$  decay information directly to extract the  $\rho_{00}$  parameter from the AMPT model and obtained consistent values as those extracted from the background subtraction method.

When there are no phase space cuts on particles (i.e. when we have full coverage), we have found that the ex-

tracted  $\rho_{00}$  or  $p_H$  value is consistent with the input value as expected. However, the experimental acceptance is always limited. The detected  $\eta$  range for final state particles is typically from  $\pm 0.5$  to  $\pm 2$ , e.g., the STAR experiment covers  $|\eta| < 1$ ; and the  $p_T$  of detected particle tracks is typically larger than 0.1 - 0.2 GeV/c. Not only are the candidate decay daughters for  $\phi$  and  $\Lambda$  reconstructions within a certain  $\eta$  and  $p_T$  coverage, but additional  $y$  (or  $\eta$ ) and  $p_T$  cuts are also often applied to the reconstructed parent particles ( $\phi$  and  $\Lambda$ ). Therefore we need to investigate whether and how the phase-space cuts may influence the extracted value of the global polarization/spin-alignment parameters. Note that the vorticity in a nuclear collision depends on the transverse position and pseudorapidity in principle[14], thus the real polarization may depend on the phase space variables such as  $\eta$  and  $p_T$ ; but that is outside the scope of this study.

*Results.* Figure 1 shows the AMPT model results for the extracted  $\rho_{00}$  of  $\phi$  mesons as a function of the upper limit of the  $|\eta|$  coverage,  $\eta_{\max}$ , for Au+Au collisions at  $\sqrt{s_{NN}} = 200$  GeV. Results are shown for two input  $\rho_{00}$  values, 0.2 and  $1/3$ , where we study the  $\eta$ -cut effects by applying the cut  $|\eta| < \eta_{\max}$  to both kaons and  $\phi$  mesons (open circles), only kaons (triangles), or only  $\phi$  mesons (stars). We see that, when the  $|\eta|$  cut is only applied to the parent  $\phi$  mesons, the extracted  $\rho_{00}$  has almost no deviation from the input value for any  $\eta$  cut. On the other hand, the extracted  $\rho_{00}$  strongly depends on the  $\eta$  cut applied to the decay daughter candidates, where an  $\eta$  coverage narrower than  $\sim 1$  gives a significantly larger extracted  $\rho_{00}$  than the input value. This is because, with the angular momentum  $\mathbf{L}$  in the transverse plane, a narrow  $\eta$  cut on kaons tends to exclude some kaons along the beam directions and thus excludes those  $\phi$ -meson decays with daughter kaons around  $\theta^* \sim 90^\circ$ . Note that such loss of decay daughters close to the beam direction due to finite acceptance and its effect on the hyperon global polarization parameter  $p_H$  have been pointed out earlier for  $\Lambda$  decays [8]. Also shown in Fig. 1 are the results where both the  $\eta$  cuts and the STAR  $p_T$  cuts ( $p_T^K > 0.1$  GeV/c and  $0.4 < p_T^\phi < 3$  GeV/c) are applied to the kaons and  $\phi$  mesons (filled circles), where we see that the  $p_T$  cuts lead to a small reduction of the extracted  $\rho_{00}$  values. We also see in Fig.1 that the extracted  $\rho_{00}$  value converges to the input value at large  $\eta_{\max}$  for all the considered cuts.

To further illustrate the  $\eta$ -cut effect on  $\rho_{00}$ , we also use a toy model, where we sample the  $p_T$ ,  $\eta$  and azimuth distributions of  $\phi$  mesons according to the AMPT results and decay the hadrons with PYTHIA [18]. As shown in Fig.2a, the effects of  $\eta$  cuts from the toy model are essentially the same as those from the AMPT model. Figure 2b shows the two-dimensional distribution (in  $\cos\theta^*$  and  $p_T$ ) of kaons within  $|\eta| < 0.3$  from  $\phi$  decays. We can clearly observe that the  $\eta$  cut excludes more kaons from  $\phi$  decays around  $\theta^* \sim 90^\circ$ , i.e., around  $\cos\theta^* \sim 0$ . The figure also demonstrates that the  $\eta$ -cut mostly affects the

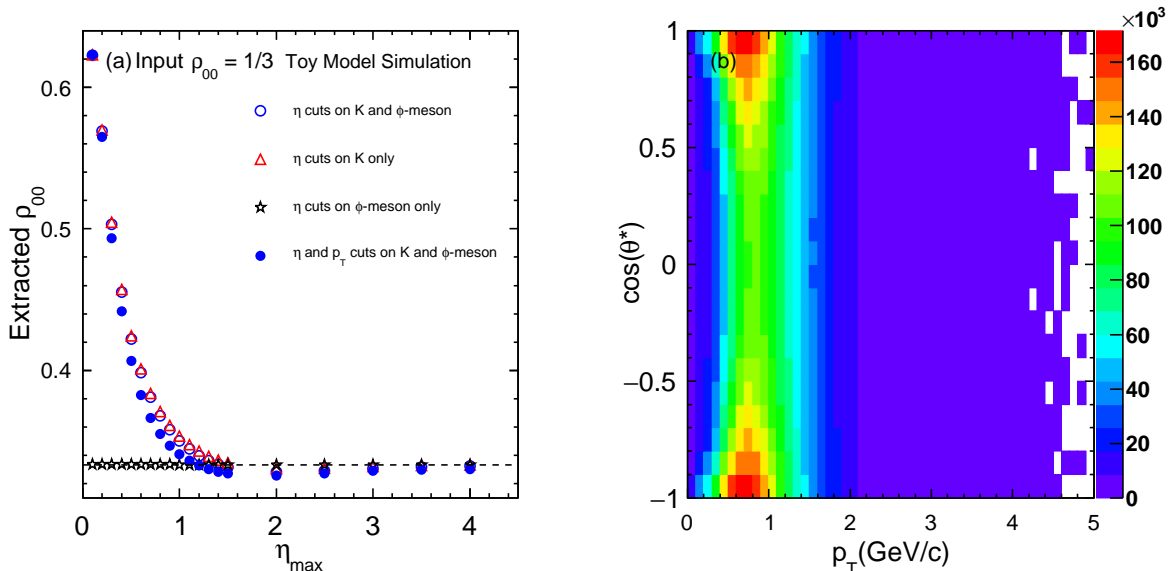


FIG. 2. (Color online) Effects of  $\eta$  and  $p_T$  cuts on  $\rho_{00}$  for  $\phi$ -meson decays from the toy model. (a) The extracted  $\rho_{00}$  as a function of  $\eta_{\max}$ . (b) Distribution in  $\cos\theta^*$  and  $p_T$  for kaons from  $\phi$  decays after applying the cut  $|\eta| < 0.3$  to kaons.

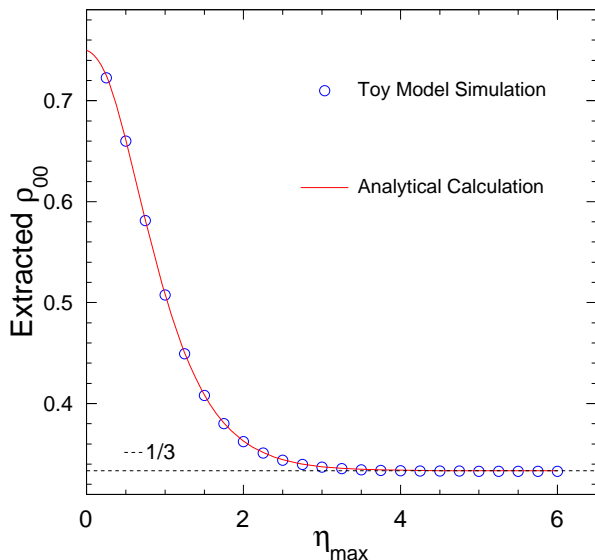


FIG. 3. (Color online) The extracted  $\rho_{00}$  as a function of  $\eta_{\max}$  for  $\phi$  mesons at rest from the toy model (circles) and analytical calculations (solid line).

low  $p_T$  region. Furthermore, a different  $\eta$ -cut effect is observed for  $\eta_{\max}$  roughly between 1.3 and 4 from both AMPT and the toy model, where the extracted  $\rho_{00}$  can be smaller than the input value. This could be the result of the finite  $p_T$  and finite anisotropic flow of the parent  $\phi$  mesons, which complicate the relation between the  $\eta$  cut

(in the center-of-mass frame) and the  $\theta^*$  distribution of the decay daughters (in the  $\phi$  rest frame). As a test, we show in Fig.3 the effect of  $\eta$  cuts on  $\phi$  mesons at rest from the toy model (circles), where the extracted  $\rho_{00}$  monotonically decreases with  $\eta_{\max}$  and finally approaches the input value ( $1/3$  here). The solid line in Fig.3 represents the analytical result on the  $\eta$ -cut effect for  $\phi$  mesons at rest, as shown in the appendix, which agrees with the toy model result.

For  $\Lambda$  hyperons, Fig.4 shows the  $\eta$ -cut effect on the  $p_H$  parameter when Eq.(3) is used to extract  $p_H$ , as often done in the experimental measurements [3, 8]. Figures 4a and 4b show the toy model results for the input value  $p_H = 0$  and  $p_H = 0.01$ , respectively; while Fig.4c shows the AMPT results for the input value  $p_H = 0.2$ . In the toy model, we sampled  $\Lambda$  hyperons using  $p_T$ ,  $\eta$  and azimuth distributions that have been fitted to the AMPT results, where the azimuth distribution includes the elliptic flow. Note that the case  $p_H = 0$  represents no real global polarization, while the case  $p_H = 0.01$  roughly corresponds to the STAR data [3]. When the input  $p_H$  is zero, we see that the extracted  $p_H$  values are consistent with zero, with or without the phase space cuts. This is in line with the expectation from the up-down symmetry with respect to the direction of  $\mathbf{L}$ . However, when the input  $p_H$  is finite (and positive), the effects of  $\eta$  cuts on  $p_H$  for  $\Lambda$  hyperons are similar as those on  $\rho_{00}$  for  $\phi$  mesons: a finite  $|\eta|$  cut applied to the decay-daughter candidates generates an extracted  $p_H$  value larger than the input value, but a finite  $|\eta|$  cut applied to parent  $\Lambda$  hyperons has little effect on the extracted  $p_H$ . Also, the extracted  $p_H$  value approaches the input value for  $\eta_{\max}$

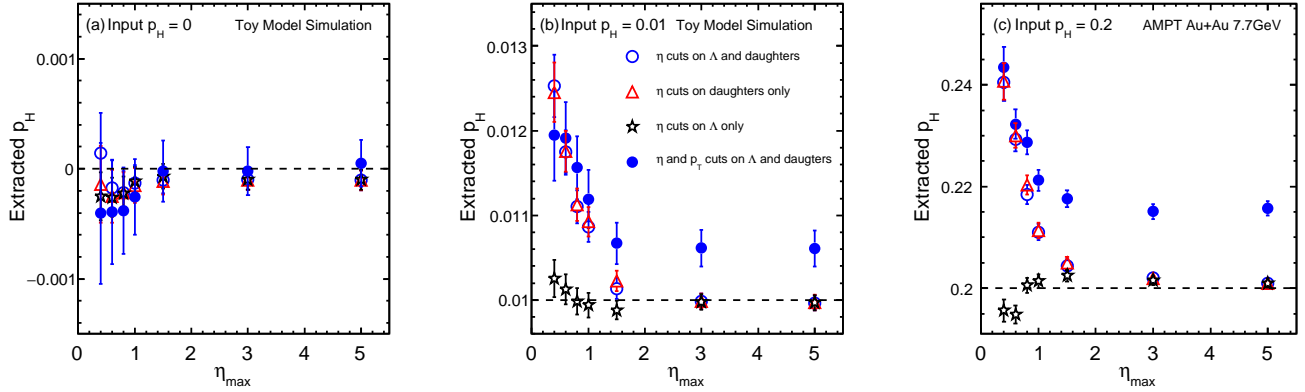


FIG. 4. (Color online) The  $p_H$  parameter extracted with Eq.(3) as a function of  $\eta_{\max}$  for Au+Au collisions at  $\sqrt{s_{NN}}=7.7$  GeV from (a) the toy model with input value of 0, (b) the toy model with input value of 0.01, and (c) AMPT with input value of 0.2. Filled circles represent the results with both  $\eta$  cuts and the STAR  $p_T$  cuts.

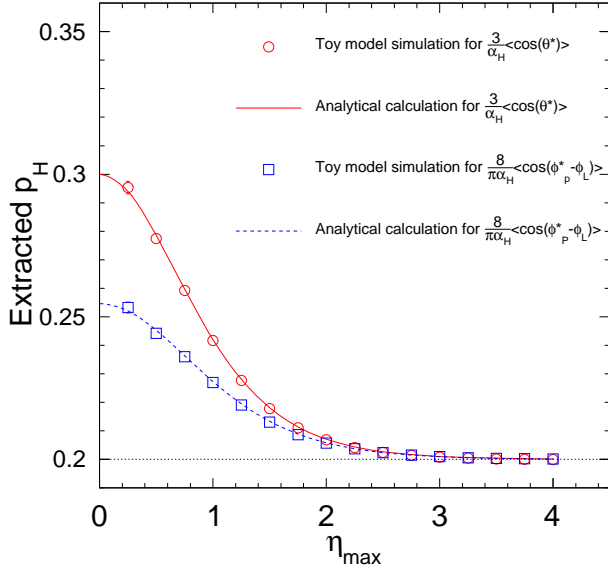


FIG. 5. (Color online) The  $p_H$  extracted with Eq.(2) (circles) or Eq.(3) (squares) as a function of  $\eta_{\max}$  from the toy model for  $\Lambda$  hyperons at rest, in comparison with the analytical results (curves), for the input value  $p_H = 0.01$  (dotted line).

greater than about 2 (when there are no  $p_T$  cuts).

We also see from Figs.4b and 4c that  $p_T$  cuts can lead to deviations of the extracted  $p_H$  from the input value, even when there is no  $\eta$  cut. This is quite different from the  $\phi$ -meson case, where the extracted  $\rho_{00}$  value is not affected by the  $p_T$  cuts when there is no  $\eta$  cut. Note that the  $p_T$  cuts in Fig.4 are the STAR cuts:  $p_T^{\text{daughter}} > 0.15$  GeV/c and  $0.4 < p_T^{\Lambda} < 3$  GeV/c. Furthermore, we see that the effects of the phase-space cuts from the AMPT

model for input  $p_H = 0.2$  in Fig.4c are qualitatively the same as those from the toy model for input  $p_H = 0.01$  in Fig.4b.

We have analytically derived the  $\eta$ -cut effect on the extracted  $p_H$  value for  $\Lambda$  decays at rest (see the appendix), which is shown as lines in Fig.5 for the input value  $p_H = 0.01$  when the  $p_H$  value is calculated with Eq.(2) (solid) or Eq.(3) (dashed). Symbols represent the corresponding results from the toy model, which agree with the analytical results. We also see that the  $\eta$ -cut effect is smaller when using Eq.(3) instead of Eq.(2).

*Discussions and summary.* While the global spin alignment and polarization signals can be respectively described by Eq.(1) and Eq.(4), phase-space cuts such as the  $\eta$  and  $p_T$  cuts discussed here modify the functional forms. We show in Fig.6 examples after the cut  $|\eta| < 0.4$  is applied, where the  $\cos\theta^*$  distribution for  $\phi$  mesons (when plotted versus  $\cos^2\theta^*$ ) and the  $\cos\theta^*$  distribution for  $\Lambda$  hyperons deviate from a straight line with a large  $\chi^2$  per degree of freedom. This method can be used in the experimental analysis to probe the effect of phase-space cuts, e.g., by selecting a narrow  $\eta$  range within the experimental coverage and observing a deviation from the expected straight line.

A natural question is whether the experimentally observed signals of spin alignment and polarization could be mostly due to the phase-space cuts. Figure 7 shows the results on the extracted  $\rho_{00}$  for  $\phi$  mesons from AMPT and the toy model for the case of no spin alignment (i.e. input  $\rho_{00} = 1/3$ ) after the STAR  $\eta$  and  $p_T$  cuts are applied. We see that the extracted  $\rho_{00}$  parameters are systematically higher than 1/3 and have a weak energy dependence, similar to the STAR preliminary measurements [4, 5]. This indicates that the effect of the phase-space cuts may be a dominant contribution to the deviation of the current experimental data of  $\rho_{00}$  from 1/3.

For  $\Lambda$  hyperons, we show in Fig.8 the toy model results from Eq.(3) for the input value  $p_H = 0$  (triangles) and

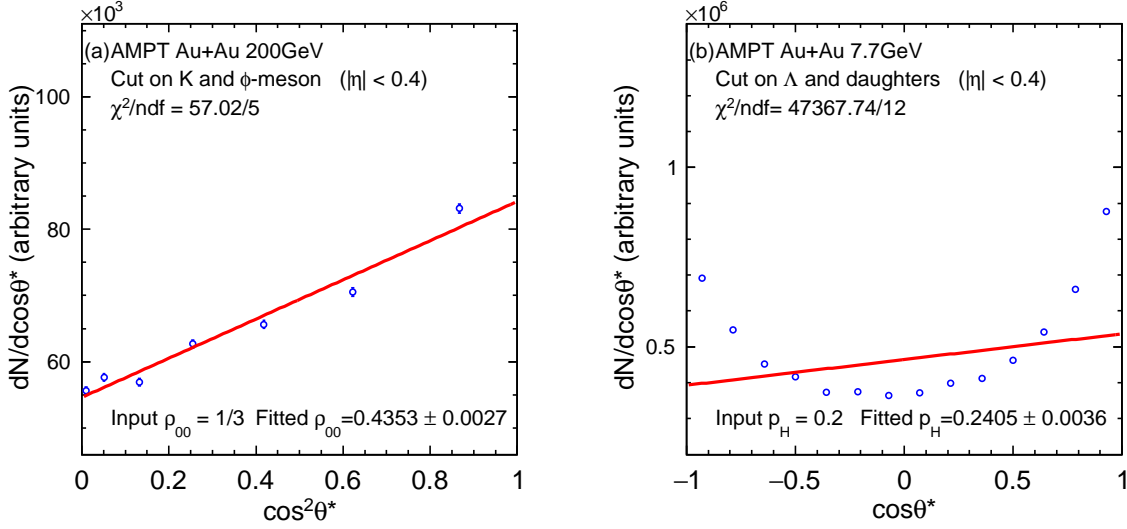


FIG. 6. (Color online) Examples of the effect of the cut  $|\eta| < 0.4$  on the shape of (a) the  $\cos^2\theta^*$  distribution for  $\phi$  mesons, and (b) the  $\cos\theta^*$  distribution for  $\Lambda$  hyperons.

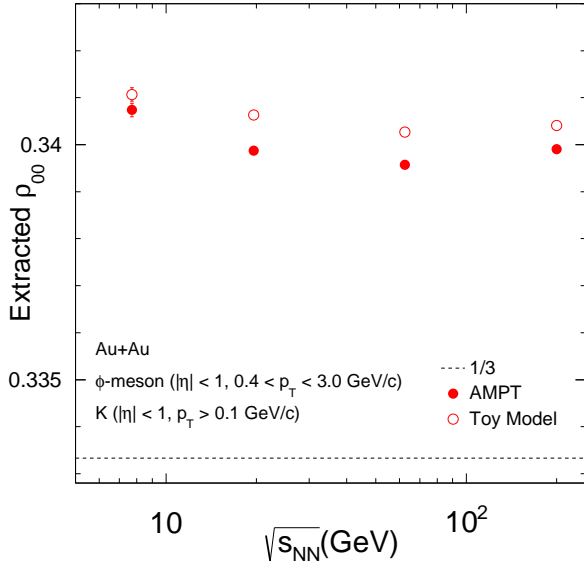


FIG. 7. (Color online) The extracted  $\rho_{00}$  of  $\phi$  mesons from AMPT and the toy model for the input value  $\rho_{00} = 1/3$  for Au+Au collisions at different energies.

$p_H = 0.01$  (squares), where the STAR phase-space cuts have been applied. We see that the extracted  $p_H$  values are consistent with zero when there is no global polarization (for input  $p_H=0$ ). With input  $p_H = 0.01$ , the extracted  $p_H$  values are rather close to the input value (within  $\sim 0.1\%$ ), and the phase-space cuts do not introduce an energy dependence for the extracted  $p_H$  values.

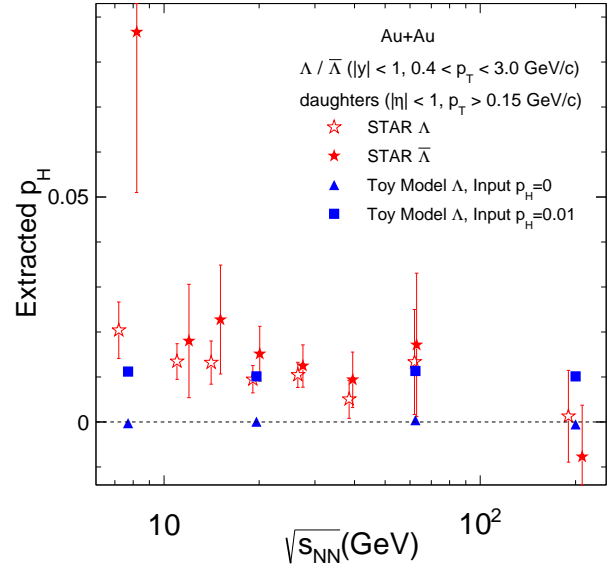


FIG. 8. (Color online) The extracted  $p_H$  of  $\Lambda$  hyperons from the toy model for the input value  $p_H = 0$  and  $p_H = 0.01$  for Au+Au collisions at different energies in comparison with the STAR data.

The STAR data [3] on the  $p_H$  values of  $\Lambda$  and  $\bar{\Lambda}$  are shown for comparisons, where the effects of phase-space cuts have already been corrected [3, 8].

In summary, we have used a modified AMPT model that includes the decays of polarized  $\phi$  mesons and  $\Lambda$  hyperons as well as a toy model to study the effects of phase-space cuts on the extracted polarization param-



ters  $\rho_{00}$  and  $p_H$ . We find that a finite  $\eta$  coverage narrower than  $\eta < \sim 1$  leads to a larger extracted value of  $\rho_{00}$  than the input value, and a similar behavior is observed for the extracted  $p_H$  when the input  $p_H$  is positive. The narrower the  $\eta$  coverage, the larger the extracted values. A finite  $p_T$  coverage also affects the extracted values of  $\rho_{00}$  and  $p_H$ . When we assume no global polarization by setting the input  $\rho_{00}$  to 1/3, the model results after the STAR  $\eta$  and  $p_T$  cuts give extracted  $\rho_{00}$  values of  $\phi$  mesons that significantly deviate from the value 1/3. These extracted  $\rho_{00}$  values are similar to the preliminary experimental data, suggesting that the phase-space cuts may be a dominant contribution to the observed higher-than-1/3 values. For  $\Lambda$  hyperons, we find that, when assuming no polarization, a finite coverage in  $\eta$  and/or  $p_T$  does not lead to a non-zero extracted  $p_H$ ; however  $\eta$  and  $p_T$  cuts affect the magnitudes of the  $\Lambda$  polarization parameter  $p_H$  when the input  $p_H$  is non-zero. Our study thus shows that measured polarization observables need to be corrected for the effects of finite acceptance before quantitative conclusions on the global polarization can be reliably made.

*Acknowledgments* We thank Mike Lisa and Nu Xu for discussions. This work was supported in part by the National Basic Research Program of China (973 program) under Grant No. 2015CB8569, National Natural Science Foundation of China under Grants No. 11628508 and No. 11475070 and China Postdoctoral Science Foundation under Grants No. 2016M592357.

## APPENDIX

In this appendix, we derive the effects of a finite  $\eta$  coverage on the extracted polarization parameters  $p_H$  and  $\rho_{00}$  for the simple case where the parent hadrons are at rest. We assume that the angular distributions of the decays, as shown in Eqs.(1) and (4), are both uniform in  $\phi^*$ , the azimuth of a daughter particle.

When a hadron decays into two daughter particles, let  $\theta^*$  be the angle between the global angular momentum  $\mathbf{L}$  and the momentum of one daughter particle, we then have

$$\cos \theta^* = \cos(\phi_p^* - \phi_{\mathbf{L}}) \sin \theta_p^*. \quad (\text{A1})$$

In the above,  $\theta_p^*$  and  $\phi_p^*$  are respectively the polar angle and azimuth of the daughter particle in the rest frame of the parent hadron. When decay daughters can only be measured within a finite  $\eta$  range  $|\eta| < \eta_{\max}$ , the range of  $\theta_p^*$  is no longer  $[0, \pi]$  but is given by

$$\theta_p^* \in [\epsilon, \pi - \epsilon], \text{ where } \epsilon = 2 \operatorname{atan}(e^{-\eta_{\max}}). \quad (\text{A2})$$

To extract the polarization parameter  $p_H$  from  $\Lambda$  decays, one can use either the average value of  $\cos \theta^*$  in

Eq.(2) or  $\cos(\phi_p^* - \phi_{\mathbf{L}})$  in Eq.(3) for the daughter protons. However, a finite  $\eta$  coverage gives the following results:

$$\begin{aligned} \langle \cos \theta^* \rangle &= \frac{\int (1 + \alpha_H p_H \cos \theta^*) \cos \theta^* \sin \theta_p^* d\theta_p^* d\phi_p^*}{\int (1 + \alpha_H p_H \cos \theta^*) \sin \theta_p^* d\theta_p^* d\phi_p^*} \\ &= \alpha_H p_H [5 - \cos(2\epsilon)] / 12, \end{aligned} \quad (\text{A3})$$

and

$$\langle \cos(\phi_p^* - \phi_{\mathbf{L}}) \rangle = \frac{\pi \alpha_H p_H}{8 \cos \epsilon} \left[ 1 + \frac{\sin(2\epsilon) - 2\epsilon}{\pi} \right]. \quad (\text{A4})$$

Therefore, when one neglects the effect of a finite  $\eta$  coverage and still uses Eq.(2), the following polarization parameter will be extracted:

$$p_H^{\text{extracted}} = p_H [5 - \cos(2\epsilon)] / 4, \quad (\text{A5})$$

which is different from the real value  $p_H$ . We can see that the extracted value in this case is always no less than the real value: it equals the real value when  $\epsilon = 0$  (full  $\eta$  coverage) but is 50% higher than the real value in the limit of zero  $\eta$  coverage. Likewise, if one neglects the effect of a finite  $\eta$  coverage and still uses Eq.(3), the extracted polarization parameter will be

$$p_H^{\text{extracted}} = p_H \left[ 1 + \frac{\sin(2\epsilon) - 2\epsilon}{\pi} \right] / \cos \epsilon. \quad (\text{A6})$$

The above extracted value is also always no less than the real value, and it is  $4/\pi$  times the real value in the limit of zero  $\eta$  coverage. The analytical results of Eqs.(A5-A6) are shown in Fig.5 and agree with the numerical results from the Monte Carlo toy model.

For  $\phi$  decays, one can use the average value of  $\cos^2 \theta^*$  to extract the polarization parameter  $\rho_{00}$ . A finite  $\eta$  coverage leads to the following:

$$\langle \cos^2 \theta^* \rangle = 1/80 \times [133 + 401\rho_{00} + (4 - 172\rho_{00}) \cos(2\epsilon) - 9(1 - 3\rho_{00}) \cos(4\epsilon)] / [7 + 3\rho_{00} + (1 - 3\rho_{00}) \cos(2\epsilon)]. \quad (\text{A7})$$

If there is no restriction on  $\eta$ , the above result reduces to  $\langle \cos^2 \theta^* \rangle = (1 + 2\rho_{00})/5$ . However, if one still uses this relation when there is a finite  $\eta$  coverage, then a different polarization parameter  $\rho_{00}$  will be extracted. In the special case of no polarization (i.e.  $\rho_{00} = 1/3$ ), we will have

$$\rho_{00}^{\text{extracted}} = \frac{1}{3} + \frac{5 \sin^2 \epsilon}{12}, \quad (\text{A8})$$

which is shown in Fig.3 and agrees with the Monte Carlo toy model results.

- 
- [1] Z.-T. Liang and X.-N. Wang, Globally polarized Quark-Gluon Plasma in noncentral  $A + A$  collisions, *Phys. Rev. Lett.* **94**, 102301 (2005).
- [2] Z.-T. Liang and X.-N. Wang, Spin alignment of vector mesons in non-central  $A + A$  collisions, *Phys. Lett. B* **629**, 20 (2005).
- [3] L. Adamczyk et. al. (STAR Collaboration), Global  $\Lambda\Lambda$  hyperon polarization in nuclear collisions: evidence for the most vortical fluid, *Nature* **548**, 62 (2017).
- [4] X. Sun for the STAR Collaboration, Collision energy dependence of  $\phi$ -meson spin alignment at the STAR experiment, *Quark Matter 2017*.
- [5] C. Zhou for the STAR Collaboration,  $\phi$  spin alignment in high energy nuclear collisions at RHIC, *Particles and Nuclei International Conference 2017*.
- [6] L. G. Pondrom, Hyperon experiments at Fermilab, *Phys. Rep.* **122**, 57 (1985).
- [7] Review of Particle Physics, *Chin. Phys. C* **38**, 090001 (2014).
- [8] B. I. Abelev et. al. (STAR Collaboration), Global polarization measurement in Au + Au collisions, *Phys. Rev. C* **76**, 024915 (2007). Erratum: *Phys. Rev. C* **95**, 039906 (2017).
- [9] B. I. Abelev et. al. (STAR Collaboration), Spin alignment measurements of the  $K^{*0}(892)$  and  $\phi(1020)$  vector mesons in heavy ion collisions at  $\sqrt{s_{NN}} = 200$  GeV, *Phys. Rev. C* **77**, 061902(R) (2008).
- [10] K. Schilling et al., On the analysis of vector-meson production by polarized photons, *Nucl. Phys. B* **15**, 397 (1970); Erratum: *Nucl. Phys. B* **18** 332 (1970).
- [11] F. Becattini, F. Piccinini and J. Rizzo, Angular momentum conservation in heavy ion collisions at very high energy, *Phys. Rev. C* **77**, 024906 (2008).
- [12] L.-G. Pang, H. Petersen, Q. Wang and X.-N. Wang, Vortical fluid and  $\Lambda$  spin correlations in high-energy heavy-ion collisions, *Phys. Rev. Lett.* **117**, 192301 (2016).
- [13] F. Becattini, L. Csernai and D. J. Wang,  $\Lambda$  polarization in peripheral heavy ion collisions, *Phys. Rev. C* **88**, 034905 (2013).
- [14] Y. Jiang, Z. W. Lin and J. Liao, *Phys. Rev. C* **94**, 044910 (2016).
- [15] Z. W. Lin, C. M. Ko, B.-A. Li, B. Zhang, and S. Pal, Multiphase transport model for relativistic heavy ion collisions, *Phys. Rev. C* **72**, 064901 (2005).
- [16] Z. W. Lin and C. M. Ko, *Phys. Rev. C* **65**, 034904 (2002).
- [17] Z. W. Lin, *Phys. Rev. C* **90**, 014904 (2014).
- [18] T. Sjostrand et. al., An introduction to PYTHIA 8.2, *Comput. Phys. Commun.* **191**, 159 (2015).